Effects of Molecular Architecture on Two-Step, Melt-Spun Poly(lactic acid) Fibers

John A. Cicero,[1] John R. Dorgan,[1] James Garrett,[2] James Runt,[2] J. S. Lin[3]

[1]*Department of Chemical Engineering, Colorado School of Mines, Golden, Colorado 80401-1887*
[2]*Department of Materials Science and Engineering, Pennsylvania State University, University Park, Pennsylvania 16802*
[3]*Solid State Division, Oak Ridge National Laboratory, Oak Ridge, Tennessee 37831*

Received 7 December 2001; accepted 1 April 2002

ABSTRACT: Fibers of poly(lactic acid) (PLA) produced by two-step melt spinning have been studied. The PLA resins used contain a 96:04 ratio of L:D stereochemical centers; however, one of the materials is branched by a peroxide treatment. The thermal, mechanical, and morphological properties of the fibers are compared for the two different molecular architectures. In the branched material, at least some of the branches exceed the entanglement molecular weight. The branched material is accordingly characterized by greater shear and extensional viscosity than the linear material. Fiber properties are highly influenced by the draw ratio; both branched and linear materials reach a plateau of about 35% crystallinity. The branched polymer reaches the plateau at a lower draw ratio, and this is indicative of faster crystallization kinetics. Both materials shrink in boiling water, and the amount of shrinkage decreases with increasing draw ratio. At an intermediate draw ratio of 6, the branched material is characterized by significantly larger shrinkage. With small-angle X-ray scattering and atomic force microscopy, the morphology is found to be fibrillar. Microfibril diameters range from approximately 20 to 30 nm and are almost identical for the two molecular architectures studied.
 J Appl Polym Sci 86: 2839–2846, 2002

Key words: fibers; melt; morphology

INTRODUCTION

Until now, the main applications of poly(lactic acid) (PLA) have been in the biomedical field. However, PLA is currently receiving attention because of its production from renewable, rather than petrochemical, sources. A polyester, PLA exhibits a number of advantages: (1) availability from renewable resources, (2) reductions in carbon dioxide emissions in comparison with conventional petroleum-based commodity plastics, and (3) significant property advantages over other materials. Cargill Dow is operating its first 300-million-pound-per-year PLA production plant in Blair, NE. Target markets for PLA include packaging, film, and textile fibers.

Because the PLA monomer possesses chirality, the stereochemistry of the polymer may be tailored with specific goals in mind. The lactide monomer may contain identical stereocenters (L:L or D:D) or enantiomeric stereocenters (L:D). Specialized catalysts hold the promise of controlling both isotactic and syndiotactic contents with different enantiomeric units.[1] Copolymers of various L:D compositions can be synthesized from mixtures of the monomers. L units are usually present in greater amounts than D units. Because the D units are basically defects in an L chain, fully amorphous materials can be made by the inclusion of relatively high D contents (>20%), whereas highly crystalline materials are obtained when the D content is low (<2%).

Solution-spun fibers of PLA, typically containing 100% L isomer, have been widely studied, especially for biomedical applications.[2–8] A focus on high strength and high modulus permeates the literature, primarily because PLA fibers are traditionally used for sutures. However, these polymer resins generally have a very high molecular weight, are costly, and spinning speeds are low.

Melt-spun fibers have been explored as well.[3,9–13] A range of production rates have been studied, from a few meters to a few thousand meters per minute. Some groups have geared these fibers toward biomedical applications, whereas others have aimed at producing fibers suitable for the textile industry. As with the solution-spun fibers, however, the PLA used is typically 100:0 L:D, of very high molecular weight, and expensive (e.g., the Purac brand materials).

Another article[14] examines in detail the effects of the temperature and draw ratio (DR) on the properties of

Correspondence to: J. R. Dorgan (jdorgan@mines.edu).
Contract grant sponsor: Agriculture Industries of the Future Program, Office of Industrial Technologies, U.S. Department of Energy; contract grant number: DE-FC07-99CH11010.

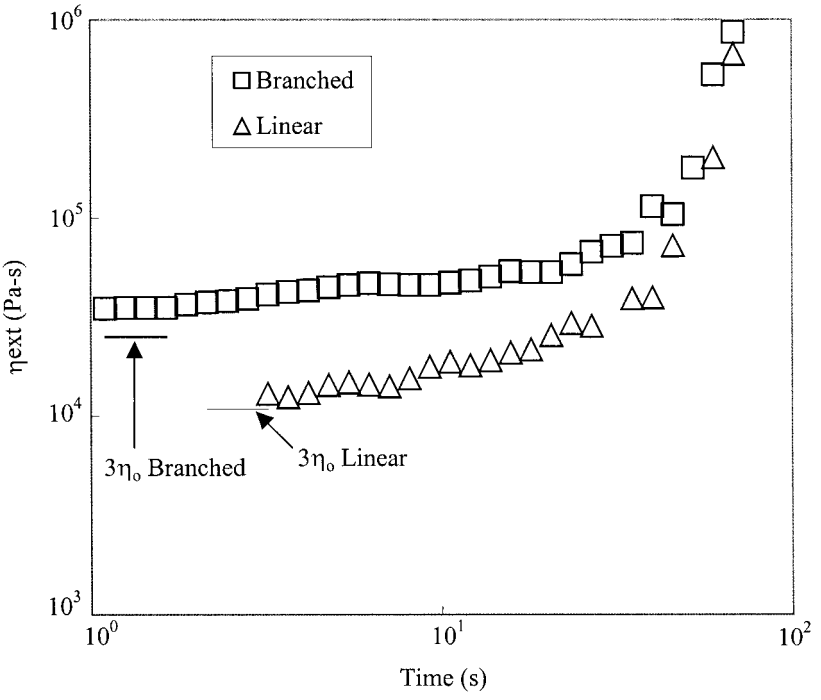

Figure 1 Growth of the elongational viscosity (η_{ext}) versus time for branched and linear molecular architectures of PLA with an L:D ratio of 96:04. The strain rate is 0.1 s^{-1}.

textile-grade PLA fibers with an L:D ratio of 98:02.[12] However, no present literature is available concerning melt-spun fibers of differing molecular architectures. The focus of this work is the combined effects of the molecular architecture and processing conditions on the thermal, mechanical, and morphological properties of melt-spun fibers produced from 96:04 L:D PLA.

MATERIALS AND METHODS

The commercial-grade PLA used in this study was provided by Cargill Dow (Minnetonka, MN) and contained an L:D ratio of approximately 96:04. The polymer was synthesized by melt polymerization in the presence of a stannous octoate catalyst. Two molecular architectures, one linear and one branched, were used. Branching was achieved by the reactive extrusion of linear PLA, initiated by peroxide.[1] For further details, the reader is referred to a review of PLA chemistry.[16] On the basis of zero-shear viscosity measurements, the branch lengths were long enough to entangle.[1,17] As measured by light scattering, initial number-average and weight-average molecular weights for the linear material were M_n = 67,300 and M_w = 110,800, respectively, whereas those for the branched material were M_n = 57,400 and M_w = 131,200. Before processing, the pellets were dried by being spread in a 1-in.-thick layer in the bottom of a stainless steel pan, which was placed in a convection oven at 82°C overnight (ca. 14 h). Expected water concentrations after drying were 100 ppm.[18]

Fibers were prepared by a two-step melt-spinning process, which is detailed in another article.[14] The apparatus consisted of a Killion KL-125 single-screw extruder mated to a pilot-scale Killion monofilament line. In this study, DR refers to the cold-draw ratio, defined as the ratio of the velocity at the take-up winder to the velocity at the beginning of the cold-draw region. The nip roller and take-up winder speeds were adjusted to keep a slight tension on the fiber.

The molecular weights of the starting resin and spun fibers were determined with light scattering, with tetrahydrofuran as the solvent. The molecular weight loss (MW loss) during processing was defined as

$$\text{MW loss} = \frac{M_{wr} - M_{wf}}{M_{wr}} \times 100\% \qquad (1)$$

where M_{wr} and M_{wf} are the weight-average molecular weights of the resin and fiber, respectively.

Extensional viscosity measurements of the branched and linear PLA resins were carried out on a Rheometrics RME instrument. Molded rectangular bars (ca. 54 mm × 8 mm × 2 mm) were tested at 180°C and an extensional strain rate of 0.1 s^{-1}. The actual strain rate was determined by video recordings of the tests per a protocol developed under a round-robin evaluation of the accuracy of the instrument.[19]

A PerkinElmer DSC 7 was used for differential scanning calorimetry (DSC) scans. The instrument was

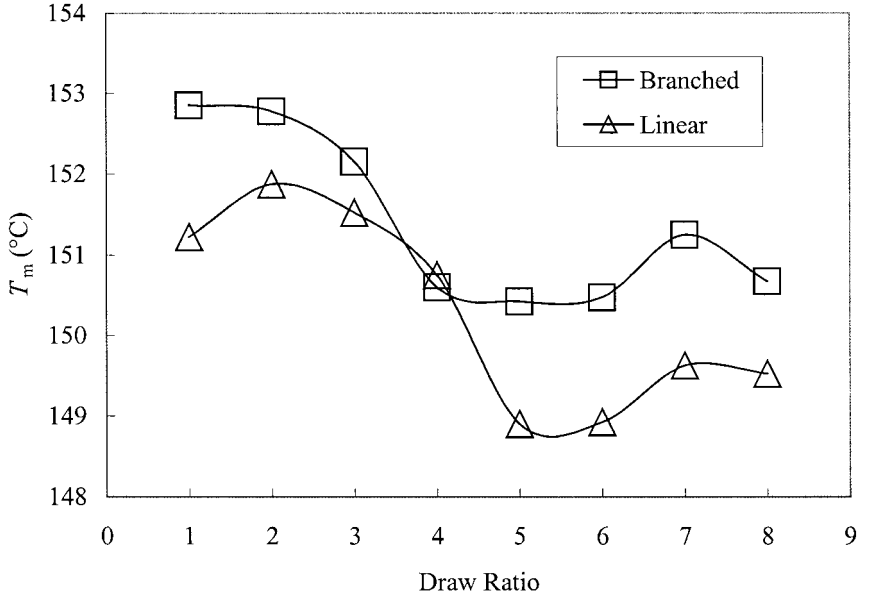

Figure 2 T_m as a function of DR.

calibrated with an indium standard before each set of analyses. Samples were prepared by fibers being cut into pieces 2–4 mm long, dried in a vacuum oven at 40°C overnight, and placed into aluminum pans (ca. 10 mg per pan). The samples were ramped to 120°C at the maximum rate (ca. 1000°C/min) to minimize recrystallization during heating and then were scanned up to 200°C at a rate of 15°C/min.

Shrinkage in boiling water experiments was performed by the selection of five fibers at random from DRs of 4, 6, and 8 for both branched and linear materials. Their original lengths were measured. The fibers were then submerged in boiling water (the bath was at 93°C because of the high altitude) for 15 min. After the fibers were removed from the bath, the length of each fiber was again measured. The shrinkage percentage was defined as

$$\text{Shrinkage (\%)} = \frac{l_0 - l}{l_0} \times 100\% \qquad (2)$$

where l_0 and l are the lengths of the original and shrunk fibers, respectively. The results were reported as the averages of five fibers for each DR.

The mechanical properties were measured with an Instron tensile testing device fitted with fiber fixtures. Specimens 2-in. long were tested at a crosshead speed of 1.2 in./min with a 2-kg load cell. Diameters were measured with an optical microscope and LECO im-

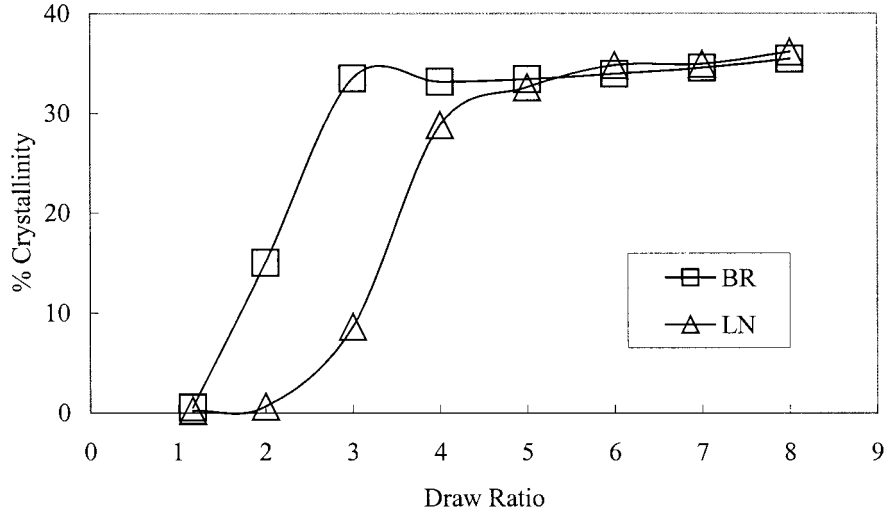

Figure 3 Crystallinity percentage as a function of DR. Faster crystallization kinetics for the branched material allow the plateau to be reached at a lower DR than for the linear PLA.

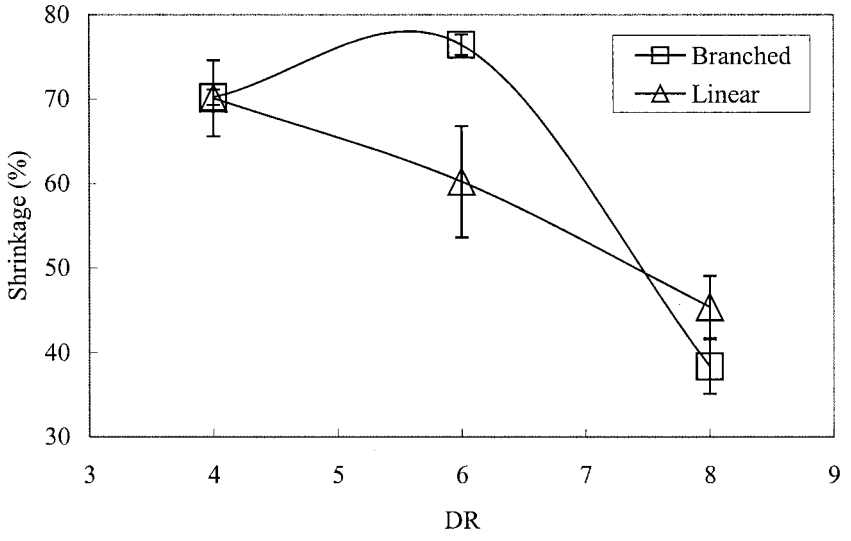

Figure 4 Shrinkage in boiling water versus DR.

age analysis software after calibration. The results were reported as averages of 10 tests for each sample.

Small-angle X-ray scattering (SAXS) and atomic force microscopy (AFM) were employed to examine the morphology of the PLA fibers. SAXS runs were made at the Oak Ridge National Laboratory. The fiber samples were carefully wrapped around an aluminum frame and mounted vertically. The sample-to-detector distance was 5.12 m.

A Digital Instruments NanoScope IIIa AFM instrument operating in the tapping mode (height and phase) was employed. To prepare each sample, a razor blade was used to make a notch nearly parallel to the fiber axis. The fiber was then pulled apart longitudinally to reveal an unscratched inner surface. An approximately 1-cm-long section of the shed fiber was placed on a magnetic AFM disk with double-sided tape. Optimum accuracy was ensured with a low scanning rate of 0.7 Hz. Typical amplitude set points ranged from 0.4 to 0.8 V. Silicon Nanoprobe tips with resonant frequencies near 330 kHz were used.

RESULTS AND DISCUSSION

Data from the linear and branched PLA are described in this section. For each molecular architecture, fibers formed from eight different DRs (1–8) are studied.

Various grades of PLA are known to exhibit significant strain hardening in response to elongational deformations.[20] A comparison of the extensional viscosities of the branched and linear materials with an L:D ratio of 96:04 is presented in Figure 1. Values for three times the zero shear viscosity are also indicated and show an approximate correspondence with the extensional viscosity at early times (i.e., the Trouton ratio is near the expected value of 3). The branched PLA

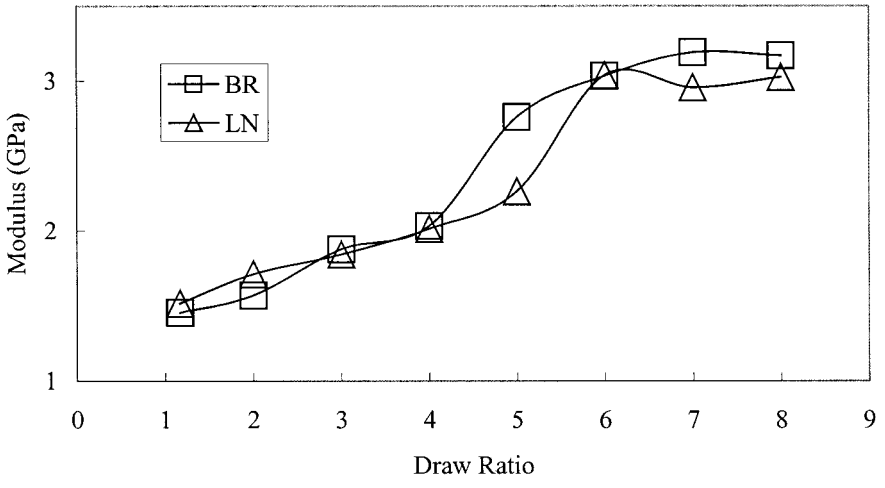

Figure 5 Modulus as a function of DR. Both branched and linear materials exhibit a large improvement in the modulus between DRs of 4 and 6.

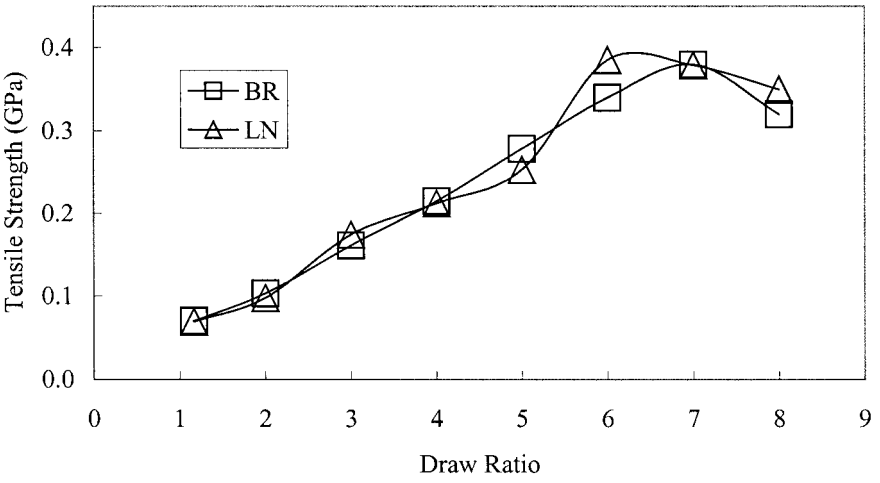

Figure 6 Tensile strength as a function of DR. The weakening at very high DRs is attributed to crazing, which has developed as a result of the high stress on these fibers during drawing.

demonstrates a higher viscosity than the linear PLA, and the higher molecular weight and long-chain branching yield longer relaxation times than in the linear counterpart.[17] Strain hardening is generally exhibited when the strain rate is much larger than the rate of molecular relaxation,[21] so one would expect the branched material to strain-harden earlier than the linear material. This is exactly what is observed in the data. The strain hardening exhibited by both branched and linear materials is favorable for fiber spinning.

Because of the rapid thermal degradation of PLA, MW loss during processing is an important issue. A 39% MW loss is seen for the linear PLA, whereas that for the branched PLA is 42%. One of the main degradation mechanisms for PLA is hydrolysis. Consequently, MW loss is highly affected by moisture content. MW loss is independent of both the day on which the material is processed and the DR. Therefore, it appears that nearly all of the degradation occurs in the extruder and is independent of the specific day of drying. Accordingly, if the degradation is due to hydrolysis, it must come from the residual water level of approximately 100 ppm. Under these conditions, a greater loss percentage is expected for higher molecular weight materials. The branched material, with a higher initial molecular weight, degrades to a greater extent than the linear material.

DSC shows no significant difference in the melting behaviors between the branched and linear PLA fibers. The melting temperature (T_m) is taken as the temperature at the maximum of the melting endotherm. Melting peaks for the branched material are 150–153°C, whereas the range for the linear material is 149–152°C. An interesting correlation between T_m and DR is presented in Figure 2. T_m passes through a maximum at DR = 2 and a minimum at DR = 5 for both molecular architectures. A similar trend is exhibited for fibers produced from PLA with an L:D ratio of 98:02.[14] Lamellar thickness (L) is related to T_m through the Gibbs–Thomson equation:[22,23]

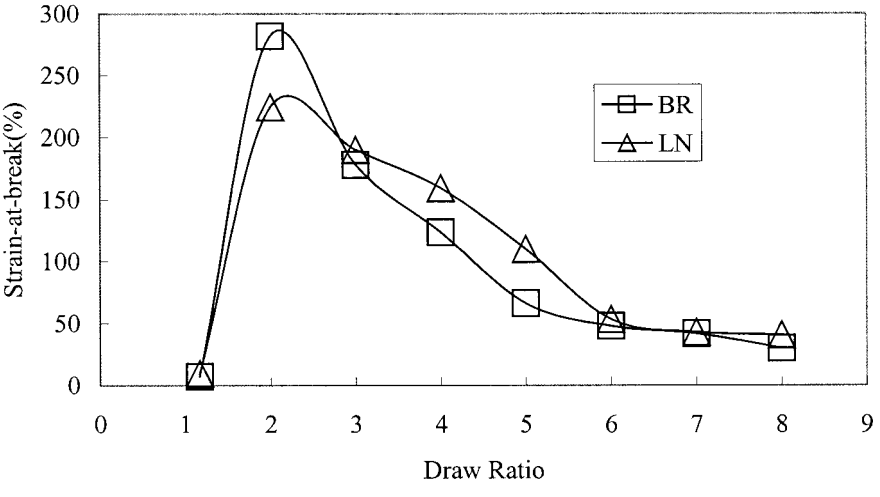

Figure 7 Strain at break as a function of DR.

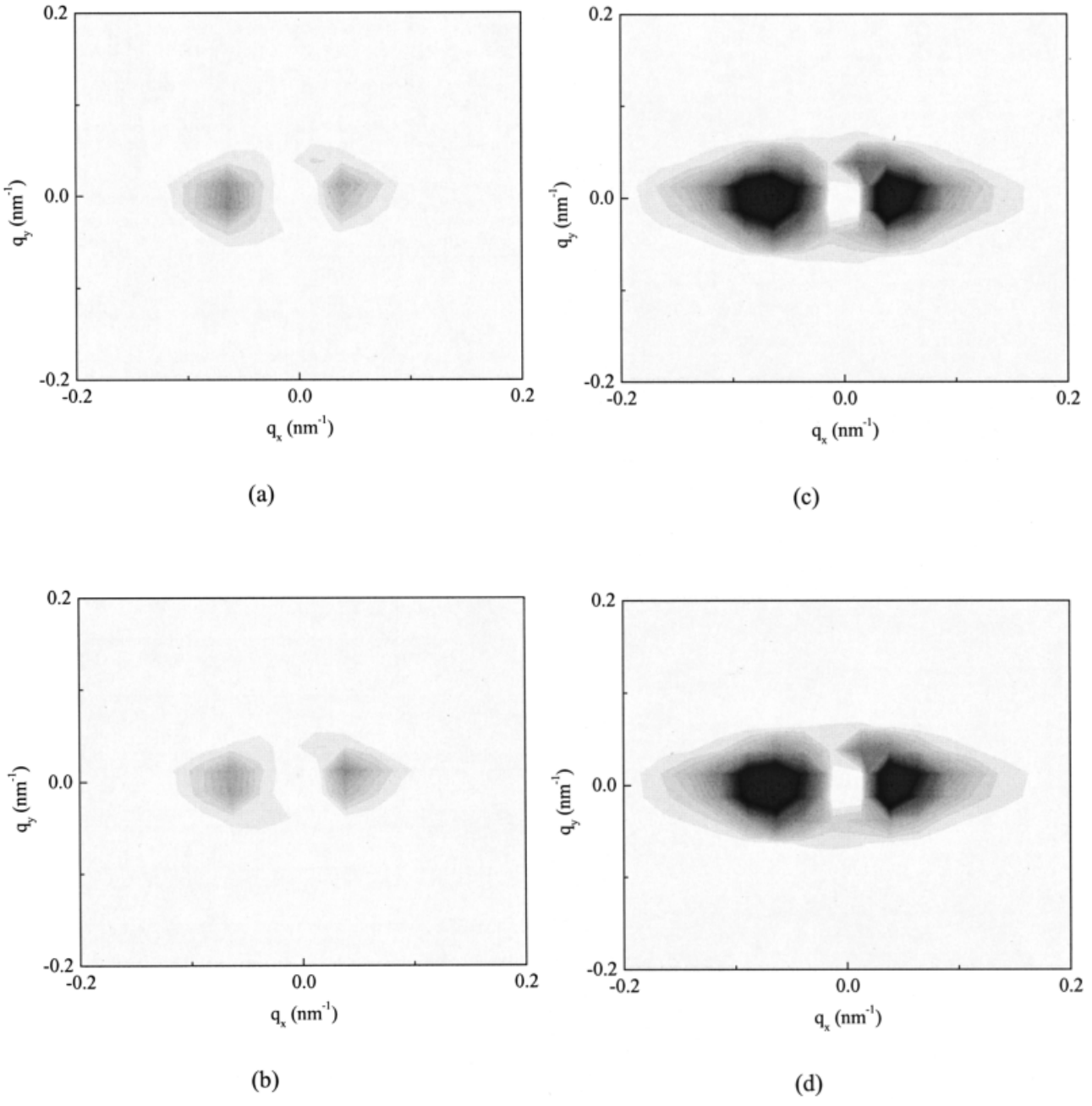

Figure 8 SAXS patterns for (a) branched PLA at DR = 2, (b) linear PLA at DR = 2, (c) branched PLA at DR = 8, and (d) linear PLA at DR = 8. The fiber axis is vertical. The equatorial scattering implies fibrillar morphology.

$$L = \frac{2\sigma_e}{\Delta H_f(1 - T_m/T_m^o)} \tag{3}$$

where σ_e is the surface free energy per unit area, ΔH_f is the melting enthalpy per unit volume of an infinite single crystal, T_m^o is the melting temperature of the infinite single crystal, and T_m is the observed melting temperature. For PLA with an L:D ratio of 96:04, σ_e = 37 mJ/m^2, ΔH_f = 93.6 J/g = 1.16 × 10^8 J/m^3, and T_m^o = 187°C.[24] L lies in the range of 7–9 nm for the two materials.

Figure 3 presents a plot of the crystallinity percentage versus DR. The crystallinity percentage is determined by the division of the area under the melting endotherm by a value of 93.6 J/g for 100% crystalline PLA.[25] Crystallinity reaches a plateau of about 35% for both molecular architectures, but the branched material reaches the plateau sooner (at DR = 3 as opposed to DR = 5 for the linear material). Quiescent crystallization in DSC demonstrates that the crystallization kinetics for the branched material are faster than those of the linear material.[1] The greater crystallinity at

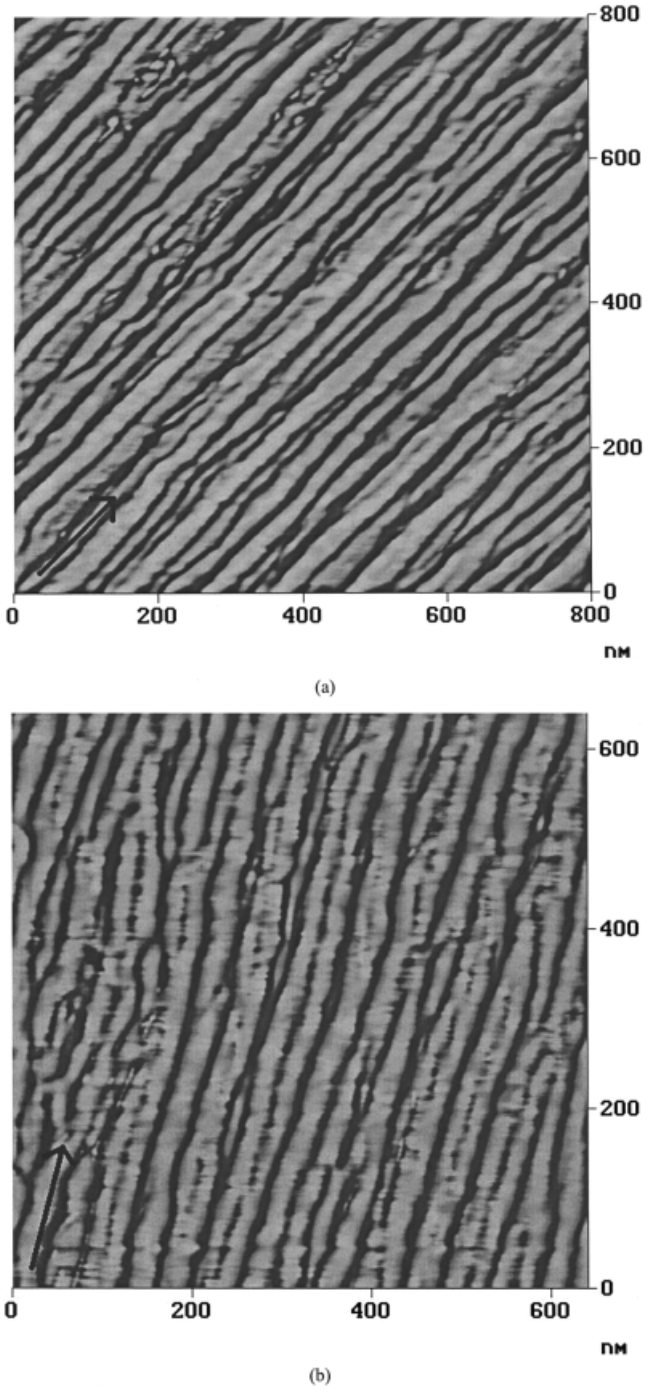

Figure 9 AFM tapping-mode height images of fibers of (a) branched and (b) linear PLA. The arrow in each image indicates the fiber axis; DRs of 6 are compared.

lower DRs for the branched material is attributed both to its intrinsically faster crystallization kinetics and to the fact that its higher viscosity produces greater stresses for the same DR, thereby facilitating a greater degree of stress-induced crystallinity.

A plot of the shrinkage in boiling water versus DR is shown in Figure 4. The branched and linear samples are very similar at DR = 4 and DR = 8, but at DR = 6, the linear material shrinks about 60%, whereas the branched material shrinks over 75%. The diameter of the latter fiber doubles during the experiment. Differences in the crystallinity percentage do not explain the observed trend; with the exception of the linear material drawn to DR = 4, all samples possess about 35% crystallinity. T_m and L similarly fail to account for the trend. The error bars in Figure 4 represent the standard deviation of the five fibers studied under each condition. Error analysis shows that measurement precision limitations are insignificant, indicating that the error bars reflect the variability in the fiber properties. The importance of these results rests in pointing out that branching can be used to increase the amount of shrinkage and that this result may be expected to carry over to the use of films in heat-sealing applications.

Figure 5 shows how modulus depends on DR. For both molecular architectures, modulus increases monotonically with DR up to a plateau value. Although the values for the branched material are generally a little higher than those of the linear material, there is essentially no difference between the two. Branching, therefore, appears to have no impact on modulus. The same can be said for tensile strength versus DR, as depicted in Figure 6. The decreases at DR = 8 are presumably due to the development of surface crazing observed at the highest DR.

A plot of the strain at break versus DR is presented in Figure 7. Here, there is a difference between branched and linear materials. The fibers spun from the branched material to a DR of 2 are extremely extensible; reproducible strains at break are 280% for the branched architecture but 220% for the linear architecture. It is not possible to say with certainty if this difference is due to molecular weight or architecture effects. However, much smaller differences are seen in modulus and strength, which are also expected to be dependent on the molecular weight. Accordingly, there is some possibility that this important physical property of the fiber can be manipulated by architectural variation in conjunction with processing steps.

SAXS patterns for DR = 2 and DR = 8 fibers of both materials are shown in Figure 8. The fiber axis is vertical. All patterns show the same kind of scattering typically seen for fibers with a fibrillar morphology.[26]

TABLE I
Microfibril Diameter Versus DR for PLA Fibers with Branched and Linear Molecular Architectures

	Microfibril diameter (nm)	
DR	Branched	Linear
4	32	30
6	19	24
8	19	23

From the SAXS patterns, it appears that both branched and linear PLA fibers exhibit fibrillar morphology, even at a DR as low as 2. Although the scattering is weak at DR = 2, it is definitely present and is equatorially concentrated. There is virtually no difference between branched and linear scattering patterns. At DR = 8, the scattering is very strong and once again concentrated equatorially. Still, no difference between the molecular architectures arises. Rough calculations give scattering object sizes of about 17 nm, but the resolution is too poor to provide accurate values. Vertical scattering (as might be caused by lamellae) is essentially nonexistent in all patterns. This is attributed to the known poor electron-density contrast between amorphous and crystalline domains of PLA.[27]

Figure 9 displays tapping-mode AFM images of the fibers produced. The arrow indicates the fiber axis in each image. Both images clearly reveal a microfibrillar network in which the microfibrils are mostly aligned with the axis. Areas in which one microfibril branches into two are seen as well as areas of connection between adjacent microfibrils. AFM shows no extraordinary difference between the fibers produced from branched PLA [Fig. 9(a)] and those produced from linear PLA [Fig. 9(b)].

Microfibril diameters for PLA fibers with a 98:02 L:D content are explored in another article.[28] Contrary to the diameters of 30–60 nm found for those fibers, the 96:04 L:D materials produce microfibril diameters that lie in the range of 19–32 nm and decrease with DR. It is presumed that the smaller microfibrils result from the smaller crystallite sizes. The higher D content limits the growth of the crystallites, which, in turn, limit the lateral dimensions of the microfibrils. Table I lists the microfibril diameters at DRs of 4, 6, and 8 for fibers of both branched and linear PLA. It is evident that the difference between the branched and linear materials is small.

CONCLUSIONS

Fibers produced from PLA at various DRs exhibit a wide range of thermal, mechanical, and morphological properties. AFM reveals that the fibrillar morphologies of the branched and linear samples are nearly indistinguishable. Molecular architecture (branched or linear) appears to have only subtle effects on fiber properties. Indications are that shrinkage and extension at break are both increased as branching is introduced. The ability to control these properties through branching may prove important in the processing of PLA films.

References

1. Dorgan, J. R.; Lehermeier, H. J.; Mang, M. J Polym Environ 2000, 8, 1.
2. Fambri, L.; Pegoretti, A.; Mazzurana, M.; Migliaresi, C. J Mater Sci Mater Med 1994, 5, 679.
3. Eling, B.; Gogolewski, S.; Pennings, A. J. Polymer 1982, 23, 1587.
4. Gogolewski, S.; Pennings, A. J. J Appl Polym Sci 1983, 28, 1045.
5. Horacek, I.; Kalisek, V. J Appl Polym Sci 1994, 54, 1751.
6. Leenslag, J. W.; Gogolewski, S.; Pennings, A. J. J Appl Polym Sci 1984, 29, 2829.
7. Leenslag, J. W.; Pennings, A. J. Polymer 1987, 28, 1695.
8. Hoogsteen, W.; Postema, A. R.; Pennings, A. J.; ten Brinke, G.; Zugenmaier, P. Macromolecules 1990, 23, 634.
9. Fambri, L.; Pegoretti, A.; Fenner, R.; Incardona, S. D.; Migliaresi, C. Polymer 1997, 38, 79.
10. Incardona, S. D.; Fambri, L.; Migliaresi, C. J Mater Sci Mater Med 1996, 7, 387.
11. Schmack, G.; Tandler, B.; Vogel, R.; Beyreuther, R.; Jacobsen, S.; Fritz, H.-G. J Appl Polym Sci 1999, 73, 2785.
12. Mezghani, K.; Spruiell, J. E. J Polym Sci Part B: Polym Phys 1998, 36, 1005.
13. Yuan, X.; Mak, A. F. T.; Kwok, K. W.; Yung, B. K. O.; Yao, K. J Appl Polym Sci 2001, 81, 251.
14. Cicero, J. A.; Dorgan, J. R. J Polym Environ 2001, 9, 1.
15. Carlson, D.; DuBois, P.; Nie, L.; Narayan, R. Polym Eng Sci 1998, 38, 311.
16. Hartmann, M. H. In Biopolymers from Renewable Resources; Kaplan, D. H., Ed.; Springer-Verlag: Berlin, 1998; p 367.
17. Lehermeier, H. J.; Dorgan, J. R. Polym Eng Sci 2001, 41, 2172.
18. Witzke, D. R. Ph.D. Thesis, Michigan State University, 1997.
19. Schulze, J. S.; Lodge, T. P.; Macosko, C. W. Rheol Acta, submitted.
20. Palade, L.-I.; Lehermeier, H. J.; Dorgan, J. R. Macromolecules 2001, 34, 1384.
21. Kasehagen, L. J.; Macosko, C. W. J Rheol 1998, 42, 1303.
22. Alberola, N.; Cavaille, J. Y.; Perez, J. J Polym Sci Part B: Polym Phys 1990, 28, 569.
23. Hoffman, J. D.; Davis, G. T.; Lauritzen, J. I. Treatise on Solid State Chemistry; Plenum: New York, 1976; Vol. 3.
24. Huang, J.; Lisowski, M. S.; Runt, J.; Hall, E. S.; Kean, R. T.; Buehler, N.; Lin, J. S. Macromolecules 1998, 31, 2593.
25. Fischer, E. W.; Sterzel, H. J.; Wegner, G. Kolloid Z Z Polym 1973, 980.
26. Grubb, D. T.; Prasad, K.; Adams, W. Polymer 1991, 32, 1167.
27. Runt, J. Pennsylvania State University, personal communication.
28. Cicero, J. A.; Dorgan, J. R. J Appl Polym Sci 2002.